

# On the Development of Quantum Mechanical Solvent Effect Models. Microscopic Electrostatic Contributions

Jane Hylton McCreery, Ralph E. Christoffersen,\* and George G. Hall

Contribution from the Department of Chemistry, University of Kansas, Lawrence, Kansas 66045. Received January 12, 1976

**Abstract:** A point charge model that conserves monopole and dipole molecular moments is applied to establishing points of hydration of a single water molecule to formamide. These studies are applied to ab initio molecular fragment as well as other ab initio and point-charge studies on the same system. In general, the shapes of point-charge potential curves are found to parallel the corresponding ab initio molecular fragment curves, except for overemphasis of the degree of stabilization in the point-charge model. These results, along with the computational simplicity of the point-charge model, appear to provide a convenient and flexible tool for examination of angular degrees of freedom in microscopic solute-solvent interactions.

In the previous paper, the various kinds of interactions that might be expected between a molecule and its environment, using solvent effects on a solute as the vehicle for discussion, were described. At the "microscopic" level, where interactions of the solute with specific solvent molecules in the vicinity of the solute are involved, several kinds of interactions were identified as being of potential importance. These interactions, similar in kind to those found in other intermolecular interactions such as intermolecular hydrogen bonding,<sup>1</sup> include electrostatic, polarization, charge transfer, exchange polarization, and correlation effects.

In principle, treatment of the system of solute plus solvent molecules as a "supermolecule" and the use of Hartree-Fock theory<sup>2,3</sup> will be sufficient to describe all except correlation and temperature averaging effects. Since correlation effects are expected typically to be nondifferentiating with respect to geometric effects,<sup>4</sup> it is expected that approaches based upon the use of Hartree-Fock theory will be sufficient to describe most of the important microscopic interactions.

However, the solution in principle is, in this case, far from an acceptable solution in practice for most systems of chemical interest. The primary reason for the difficulty arises from the very large number of geometric degrees of freedom that the collection of individual solvent molecules may have, relative to the solute. Even though carrying out an SCF calculation for any particular nuclear configuration of the molecular system may be feasible and even relatively inexpensive, examination of sufficient nuclear configurations to insure location of appropriate minima corresponding to hydration sites is quite difficult, especially if multiple explicit solvent molecules are to be examined. Thus, if computational tractability is to be obtained, a model is required which, while still using microscopic properties of the solute and solvent molecules, will allow investigation of the solute-solvent supermolecule interactions with sufficient speed that exploratory investigations may include a study of a large number of nuclear configurations of the solute-solvent system.

While several types of approaches to this problem have been explored,<sup>5-18</sup> one possible approach that has satisfactory computational characteristics is based upon the use of a point-charge model of both solute and solvent molecules, based upon the quantum mechanical SCF description of the molecule. In this case, calculation of interaction energies for various angular degrees of freedom can be carried out using classical electrostatics. Several approaches using such a model have been described and applied, including studies by Bonaccorsi et al.,<sup>14</sup> Alagona et al.,<sup>15,16</sup> and Port and Pullman.<sup>17</sup>

The approach to be described here is also a point-charge model, but it is based upon the unusually fine adaptability of

floating spherical Gaussian orbitals<sup>19</sup> (FSGO) for use in point-charge models.<sup>20-22</sup> In the following sections the model is described and application to the hydration of formamide by a single water molecule is made, along with "supermolecule" SCF calculations at the corresponding geometries for comparison purposes.

## Microscopic Electrostatic Interactions Using FSGO

In order to develop a microscopic electrostatic model in which the characteristics of the quantum mechanical charge distribution are retained, it is desirable that any classical electrostatic approximation to the quantum mechanical distribution describe reasonably accurately the monopole and higher multipole characteristics of the original quantum mechanical description. In the case of FSGO basis orbitals, a point-charge description that conserves both monopole and dipole moment has been given by Hall and collaborators<sup>20,21</sup> and is well suited for convenient computations.

This model assumes a basis set of FSGO, defined as:

$$G_s(\mathbf{r}) = N_s \exp\{-(\mathbf{r} - \mathbf{R}_s)^2/\rho_s^2\} \quad (1)$$

$$= N_s \exp\{-\alpha_s(\mathbf{r} - \mathbf{R}_s)^2\} \quad (2)$$

where  $N_s$  is a normalization constant,  $\rho_s$  is the orbital radius of the FSGO,  $\mathbf{R}_s$  is the location of the origin of the FSGO relative to an arbitrary origin, and

$$\alpha_s = 1/\rho_s^2 \quad (3)$$

It is well known that the product of any two FSGO is itself an FSGO, centered at

$$\mathbf{R}_{st} = (\alpha_s \mathbf{R}_s + \alpha_t \mathbf{R}_t)/(\alpha_s + \alpha_t) \quad (4)$$

with exponent

$$\alpha_{st} = (\alpha_s + \alpha_t) \quad (5)$$

The total electron density can be written as

$$\rho(\mathbf{r}) = \sum_{s,t} P_{st} G_s(\mathbf{r}) G_t(\mathbf{r}) \quad (6)$$

where  $P_{st}$  is an element of the charge and bond order matrix resulting from the SCF calculation.

The point-charge model of Hall<sup>20,21</sup> approximates the total density by a sum of fixed point charges, i.e.,

$$\rho^*(\mathbf{r}) = \sum_{s,t} Z_{st} \delta(\mathbf{r} - \mathbf{R}_{st}) \quad (7)$$

in which the point charges are located at points  $\mathbf{R}_{st}$  and the magnitude of their charge is

$$Z_{st} = P_{st} S_{st} \quad (8)$$

where

$$S_{st} = \int G_s G_t \, d\mathbf{r} \quad (9)$$

As shown by Hall, such an approximation ( $\rho^*(r)$ ) to the actual density ( $\rho(r)$ ) has the important attribute that the approximate density conserves both molecular monopole and dipole moment and has an electrostatic potential which is the asymptotic expansion of that given by  $\rho(r)$ . Hence, such a point-charge model may be suitable for examining large numbers of angular degrees of freedom for fixed distances in a computationally convenient fashion. Of course, distance variables cannot be examined reliably using such a model without inclusion of other interactions. Finally, it should be noted that other point-charge models for FSGO are also possible<sup>22</sup> and the discussion given here is not limited to any particular choice of point-charge representation.

For comparison purposes, the studies that have been carried out using this model and are described in the subsequent sections, have also been carried out using the "supermolecule" approach, in which the solute and solvent molecules are treated as a single molecular system, using the *ab initio* SCF molecular fragment technique.<sup>23</sup>

### Characterization of Prototype Systems

In order to undertake a systematic investigation of the suitability of point-charge models formed from SCF wave functions using FSGO basis orbitals for examining angular solute-solvent interactions, a series of studies was undertaken on a system that is complex enough to contain the various kinds of interactions, but for which other studies are also available for comparison. In particular, the system consisting of a single water molecule and the formamide molecule has been chosen for study, since detailed studies using both a "supermolecule" approach and a point-charge model have been carried out by Alagona et al.<sup>16</sup> using a (7s,3p/3s) atomic Gaussian basis contracted to a minimum basis set.

To facilitate comparisons, the notation and coordinate systems were defined as in the studies of Alagona et al.<sup>16</sup> and are summarized in Figure 1.

In the calculations to be described below, the position of the oxygen nucleus of H<sub>2</sub>O relative to the carbonyl oxygen of formamide will be taken as a definition of the "configuration" of the system, while the orientation of H<sub>2</sub>O with respect to formamide will be taken as the definition of the "conformation" of the system. As indicated in Figure 1, the initial studies to be described below are ones in which the association involves two regions of interest, in both of which the water molecule serves as a proton donor in an intermolecular hydrogen bond to the formamide carbonyl group.

In particular, the configurations of interest will be specified in terms of spherical coordinates centered on the oxygen nucleus of formamide, with the *z* axis taken along the C=O axis and the *x* axis as shown.  $\vartheta$  is the polar angle and  $\phi$  is the usual

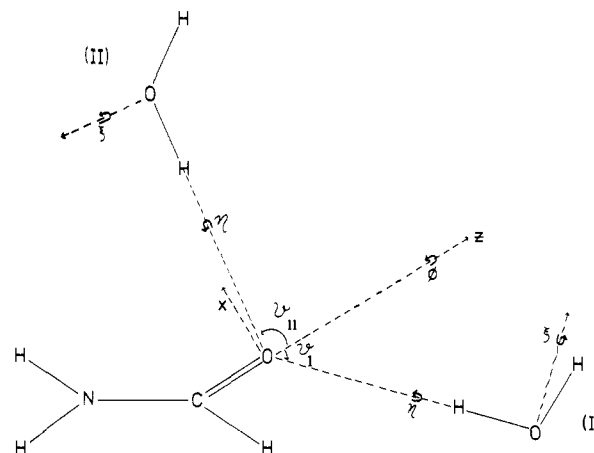


**Figure 1.** Description of two regions of formamide-H<sub>2</sub>O association and angles of rotation investigated. ( $\xi$ ,  $\eta$ ,  $\zeta$ ) form a right-handed set of axes, i.e., the positive  $\zeta$  axes point from the formamide plane upwards.

azimuthal angle, measured counterclockwise from the formamide plane. In addition, the conformations of interest are defined by means of rotations of H<sub>2</sub>O around one or more of three orthogonal axes ( $\xi$ ,  $\eta$ ,  $\zeta$ ), with origin fixed on the oxygen nucleus of H<sub>2</sub>O. As indicated in Figure 1, the  $\eta$  axis is the hydrogen bond axis, and the  $\xi$  axis is perpendicular to the  $\eta$  axis with definitions for the two regions of interest as shown. The  $\zeta$  axis is perpendicular to the ( $\xi$ ,  $\eta$ ) plane, and the positive  $\zeta$  axis is directed up from the plane when formamide and H<sub>2</sub>O are coplanar.  $\eta = 0$ ,  $\xi = 0$ , and  $\zeta = 0$  correspond to H<sub>2</sub>O being coplanar with formamide, as shown in Figure 1.

In all of the calculations, the value of *R* (the O...O distance) was fixed at 2.815 Å, one of the values employed by Alagona et al.<sup>16</sup> Also, the geometry of the individual species was kept fixed, using the crystal formamide dimer structure<sup>24</sup> and the experimental observed values for H<sub>2</sub>O, i.e., *R*(OH) = 0.957 Å and  $\angle$  HOH = 104.52°.

In the case of "supermolecule" calculations, the total basis set for the aggregate was taken simply as the combination of the basis sets for H<sub>2</sub>O and formamide. This results in a total basis of 20 orbitals (24 FSGO) for the "supermolecule" SCF calculations. To obtain starting points for the two regions of association, the H<sub>2</sub>O molecule was assumed to lie in the formamide plane so that both  $\phi$  and  $\eta$  are 0 or 180°. The results of optimization of other parameters to obtain the most stable predicted geometries for these two regions of association are presented in Table I.

To examine the variation of stabilization energy as a function of various configurations and conformations of H<sub>2</sub>O, several studies were made, using both the "supermolecule" and point-charge approach. The case of in-plane rotations involving the angle  $\vartheta$  is summarized in Figure 2. As can be seen, the minima predicted from the "supermolecule" SCF approach and the point-charge model are very similar, differing most for

**Table I.** Optimized Configurational and Conformational Parameters<sup>a</sup> for Two Formamide-Water Associations

Association	Configurational parameters			Conformational parameters			Stabilization energy, <sup>b</sup> kcal/mol
	<i>R</i> , Å	$\vartheta$	$\phi$	$\xi$	$\eta$	$\zeta$	
I. Point charge	2.815	90	180	0	0	0	9.7
SCF	2.815	90	180	0	0	0	9.6
II. Point charge	2.815	90	0	0	180	14	11.9
SCF	2.815	80	0	0	180	14	10.8

<sup>a</sup> The variables included in the optimization process were  $\vartheta$ ,  $\xi$ , and  $\zeta$ .  $\phi$  and  $\eta$  were fixed as indicated to allow comparison with the studies of Alagona et al.<sup>7</sup> <sup>b</sup> The stabilization energy is defined for the purpose of this study as:  $SE = E(\text{formamide}) + E(\text{H}_2\text{O}) - E(\text{complex})$ , where the various *E* are calculated either in an *ab initio* SCF calculation or using the point-charge approximation as described in the text.

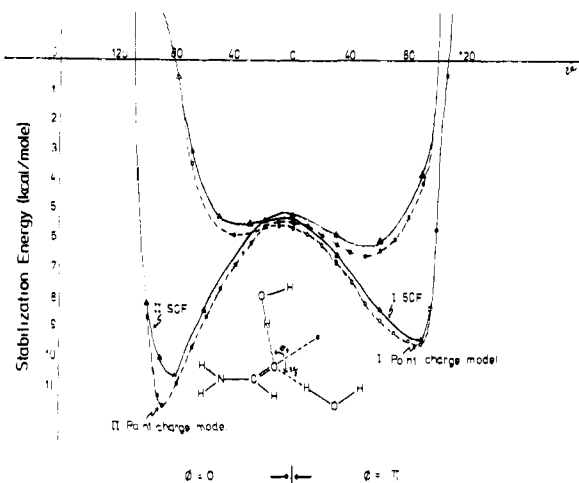


**Figure 2.** Variation of stabilization energy for in-plane rotations of  $\text{H}_2\text{O}$ . Full curves refer to "supermolecule" SCF calculations, and dashed curves refer to point charge calculations. Points to the right of  $\vartheta = 0^\circ$  refer to association I as the starting point ( $\vartheta_{11}$ ) and have  $\phi = 180^\circ$ . Points to the left of  $\vartheta = 0^\circ$  refer to association II as the starting point ( $\vartheta_{11}$ ) and have  $\phi = 0^\circ$ . In this figure,  $\xi = \eta = \zeta = 0^\circ$  were used for association I, and  $\xi = 0^\circ$ ,  $\eta = 180^\circ$ , and  $\zeta = 14^\circ$  were used for association II.

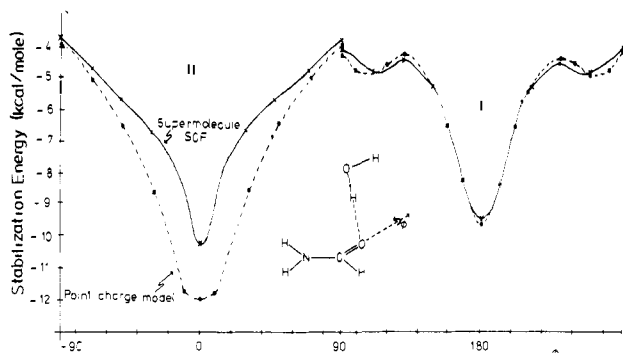


**Figure 3.** Variation of stabilization energy for configurations of  $\text{H}_2\text{O}$  above the formamide plane. See Figure 2 caption for plotting conventions.  $\xi = \eta = \zeta = 0^\circ$  and  $\vartheta = 90^\circ$  were used for association I, and  $\xi = 0^\circ$ ,  $\eta = 180^\circ$ ,  $\zeta = 14^\circ$  and  $\vartheta = 90^\circ$  were used for association II.

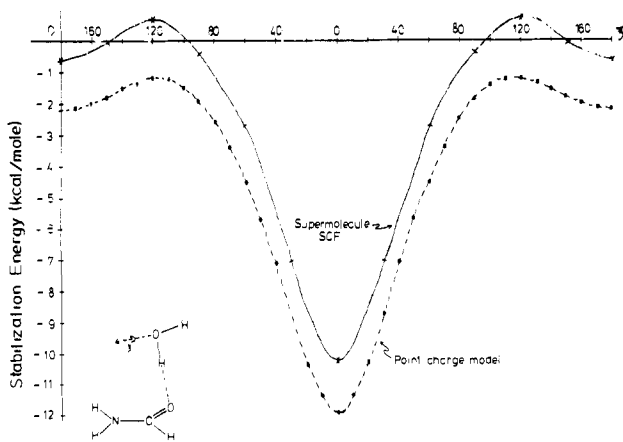


**Figure 4.** Variation of stabilization energy as a function of  $\xi$  for conformations of  $\text{H}_2\text{O}$  in the region of association II. See Figure 2 caption for plotting conventions.  $\vartheta = 90^\circ$ ,  $\eta = 180^\circ$ ,  $\zeta = 14^\circ$ , and  $\phi = 0^\circ$  were used in this study.

the case of the  $\vartheta_{11}$  variation, where a  $10^\circ$  difference in the position of the minimum is observed between the two approaches.

Figure 3 indicates the change in stabilization energy as a

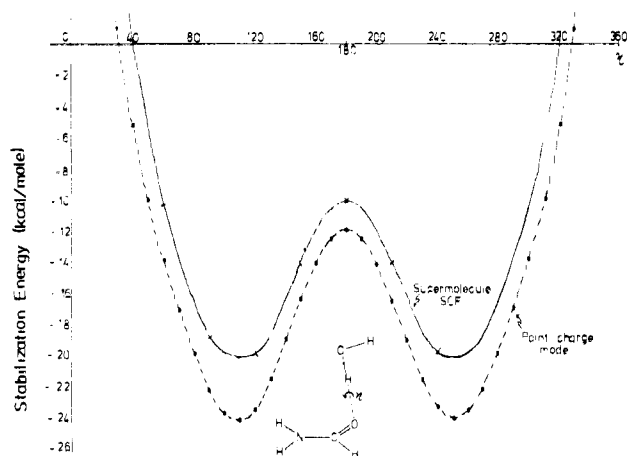


**Figure 5.** Variation of the stabilization energy as a function of  $\eta$  for conformations of  $\text{H}_2\text{O}$  in the region of association II. See Figure 2 caption for plotting conventions.  $\vartheta = 90^\circ$ ,  $\phi = \xi = 0^\circ$ , and  $\zeta = 14^\circ$  were used in this study.

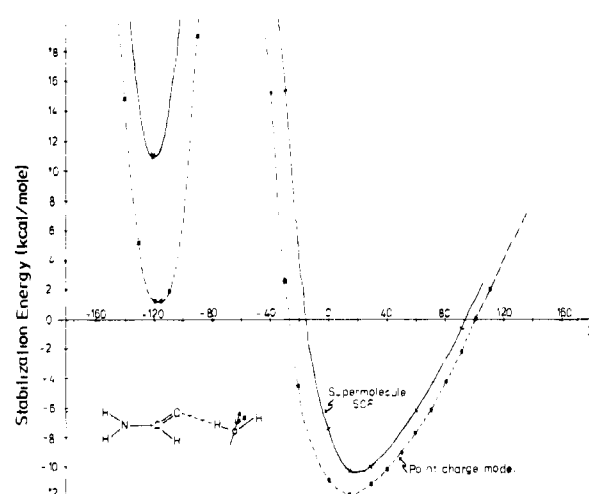


**Figure 6.** Variation of stabilization energy as a function of  $\zeta$  for conformations of  $\text{H}_2\text{O}$  in the region of association II. See Figure 2 caption for plotting conventions.  $\vartheta = 90^\circ$ ,  $\phi = \xi = 0^\circ$ , and  $\eta = 180^\circ$  were used in this study.

function of rotation of  $\text{H}_2\text{O}$  out of the formamide plane. The discontinuities observed at  $\phi = 90^\circ$  arise from starting from the association II predicted equilibrium geometry for  $\phi < 90^\circ$  and starting from the predicted association I geometry for  $\phi > 90^\circ$ . As is indicated in the figure, the position of the predicted minima are the same for both methods. Also, the general shape of the curves is quite similar, with slightly greater differences in predicted degree of stabilization occurring for regions in the vicinity of association II.

The effect of conformational changes on stabilization energy is indicated in Figures 4–6. In Figure 4 the dependence of stabilization energy on rotations about  $\xi$  for association II is described. As in Figure 3, the overall shape of the point charge and "supermolecule" SCF curves is seen to be quite similar. In particular, the position of the minimum is predicted to be the same in both approaches, although the magnitude of the predicted stabilization energy is consistently greater for the point-charge model. In Figures 5 and 6, analogous results are seen for the dependence of stabilization energy on the angles  $\eta$  and  $\zeta$ , which represent other conformational possibilities for  $\text{H}_2\text{O}$  in the region of association II. It is also of interest to note, however, that the predicted minimum in Figure 5 for rotation about  $\eta$  is for a location of the nonbonded hydrogen in  $\text{H}_2\text{O}$  at  $110^\circ$  above (or below) the formamide plane, instead of in the

plane (which was the initial starting point). Also, in Figure 6 it is of interest to note that the predicted minimum as a function of  $\zeta$  is one in which the intermolecular hydrogen bond is non-linear.

## Discussion

Before discussing the details of individual angular variation studies, several general comments are appropriate. First, the data in Figures 2–6 and Table I indicate that the particular point-charge model used here<sup>20,21</sup> provides generally a quite adequate representation of the actual SCF curves. In particular, the shapes of SCF and point-charge curves are seen to be very similar in all cases, with the point-charge model generally overemphasizing the stability of preferred conformations. The predicted minima appear usually at the same places, with the largest discrepancy occurring in the case of variation of  $\vartheta$ , where the SCF and point charge predicted minima differ by 10° (see Table I). Also of interest in this regard is that the point-charge model used here appears generally to provide a more accurate representation of the electrostatic interaction than that given by the point-charge model used by Alagona et al.<sup>16</sup> Because of this close modelling of the interaction energy by the current point-charge model and because of the known predominance of the electrostatic component in intermolecular hydrogen bonding,<sup>25</sup> the value of such a point-charge model in establishing rapidly and effectively the variation of energy with angular variables seems clear. Of course, distance variations are not expected to be usefully carried out within a point-charge model. However, considering the large number of degrees of freedom that need to be investigated when a solute plus multiple solvent molecules are considered, the usefulness and convenience of point-charge models for identification of regions of interest for angular variables cannot be overemphasized.

Comparison of the FSGO supermolecule results with those of Alagona et al.<sup>16</sup> is also of interest. In particular, the Alagona et al. study employed an (7s,3p/3s) atomic basis, contracted to a minimum basis set of 18 orbitals. The FSGO calculations employed 24 FSGO, contracted to 20 orbitals for the SCF calculations. The calculated stabilization energy is ~9.4 kcal/mol in the Alagona et al. study and  $\approx$ 10.8 kcal/mol using the FSGO basis, and the predicted structure of the complex is the same. Since both basis sets are small, overestimation of the interaction energy is expected. Enlargement of the basis would certainly reduce this effect as well as any “basis set extension effect”. Studies of the magnitude and nature of these effects are underway and judgement of the definitiveness of the studies reported here for chemical purposes must await further investigations. However, it is of interest at this point to note that both basis sets result in quite similar results, but FSGO basis orbitals are particularly convenient to handle computationally and can be used in very large molecular calculations with relative ease.<sup>26</sup>

Considering the individual angular studies in greater detail, we note that the predicted minimum for variation in  $\vartheta$  occurs in the SCF calculations at  $\vartheta = 80^\circ$  for configuration II (See Figure 2) and  $\vartheta = 90^\circ$  for configuration I. The corresponding minima using the point-charge model are 90 and 90°, respectively. For comparison purposes, the corresponding results in the study of Alagona et al. are 88 and 72° for I and II, respectively, using SCF calculations, and 60 and 67° for configurations I and II using their point charge model. Apparently, the characteristics of the point-charge model used by Alagona et al. that give rise to “too wide variation of the penetration of the van der Waals spheres as  $\vartheta$  changes”<sup>16</sup> (and led to a 28° difference in the predicted minimum energy angle ( $\vartheta$ ) between SCF and point-charge calculations for I) are not manifested as seriously in the current point-charge model. Alternatively, the conservation of total dipole moment in the current point-

charge model may be a significant improvement in the model, which is not present in the model used by Alagona et al.<sup>16</sup>

In addition, association II is found to be slightly more stable in the current studies, using either the SCF or point-charge model. On the other hand, association I is found to be most stable in the SCF calculations of Alagona et al., while their point-charge model predicts association II to be most stable. Hence, it would appear that the current point-charge model is more adequately describing the characteristics of the SCF wave function upon which it is based, and that these characteristics are of importance in the study of the energy as a function of  $\vartheta$ .

For the case of variation of energy as a function of rotation above the formamide plane (Figure 3), the shape of the SCF and point-charge curves are again seen to be quite similar, with the minimum occurring at the same angles for both configurations. For configuration II, the point-charge model predicts a deeper minima than the SCF studies. This attribute is seen throughout and is to be expected due to the general inability of point-charge models to describe the repulsions arising from delocalized electrons interacting with each other.

Considering the relative depth of the minima, it is seen that association II is favored using either the SCF or point-charge procedure. For comparison, the studies of Alagona et al. indicate the same minimum angles for the  $\phi$  variation, but find association I to be favored in the SCF study and association II to be favored using the point-charge models.

The favoring of association II in the current studies compared to the results of Alagona et al. may be due to a geometric effect. In particular, an optimum value of  $\vartheta = 72^\circ$  was used in the study of Alagona et al., while a corresponding optimum value of  $\vartheta = 90^\circ$  was used in the current study. This latter value of  $\vartheta$  brings the oxygen nucleus much closer to the NH<sub>2</sub> group, thus allowing the possibility of a second intermolecular hydrogen bond to the water molecule as a proton acceptor and the NH<sub>2</sub> group as a proton donor. This double hydrogen bonding situation would thus preferentially stabilize association II (compared to association I) and appears as a kind of composite of the associations II and III in the study of Alagona et al.

For the variation about  $\xi$  (Figure 4), the shape of the SCF and point-charge curves are seen to be quite similar, with the minimum predicted at  $\xi = 0^\circ$  in both the SCF and point-charge studies. Similar results were obtained in the studies of Alagona et al., except that their SCF curve predicts a deeper minimum than the point-charge curve.

For rotations about the angle  $\eta$  (Figure 5), the point-charge and SCF calculations are again seen to give very similar results, but striking differences are observed when comparisons are made with the studies of Alagona et al. In particular, the substantial barrier seen around  $\eta = 180^\circ$  in the current studies is completely absent from the studies of Alagona et al. However, differences in geometry may again be the source of the different shaped curves. As observed in the  $E$  vs.  $\phi$  curves, the use of  $\vartheta = 90^\circ$  in the current studies brings the oxygen of the water molecule close to the NH<sub>2</sub> group, allowing the possibility of a second intermolecular hydrogen bond. When rotation about  $\eta$  is then performed, values of  $\eta$  around 180° will bring one of the hydrogens of the water molecule into close proximity to one of the hydrogens of the NH<sub>2</sub> group. This will produce the observed barrier around  $\eta = 180^\circ$  observed in the current studies and may explain why it is not seen in the studies of Alagona et al., where  $\vartheta = 72^\circ$  was used.

Finally, for variations of energy affecting the linearity of the hydrogen bond (see Figure 6), it is again seen that the point-charge and SCF curves are quite similar, with the point-charge model again showing deeper minima. The shapes of the curves are also similar to those reported by Alagona et al., although their minima are less deep and the secondary minimum is lo-

cated at  $\xi \approx -93^\circ$  instead of  $-120^\circ$  as observed in the current studies. However, the nonlinearity of the hydrogen bond is seen in this study as well as that of Alagona et al. and at very similar minimum energy angles ( $\xi = 14^\circ$  for the SCF and point-charge curves in the current study, and  $\xi = 12$  and  $13^\circ$  for the SCF and point-charge curves, respectively, in the studies of Alagona et al.). The differences in magnitudes of the interactions in the two studies may again be due to different geometry choices ( $\vartheta = 90$  vs.  $72^\circ$ ).

In summary, the current studies reveal several points of interest. First, the shapes and positions of the minima found by the point-charge model used here are generally in good agreement with the SCF wave function upon which they are based. Thus, point-charge models may be particularly useful for investigation of intermolecular interactions involving angular variations. Second, the particular point-charge model employed, which conserves the molecular dipole as well as monopole moment, appears to reproduce the features of SCF wave functions better than other point-charge models.

It should be remembered that, when point-charge models are used, difficulties will be encountered in several situations, e.g., when charges are sharply varying functions of conformational changes or if conformational changes bring two or more point charges within approximately the sum of the orbital radii of the FSGO from which the point charges were constructed. Finally, it should be remembered that the point-charge models, while extremely useful and efficient for identifying conformational and/or configurational regions of interest, can be no better than the quality of the SCF wave function upon which they are based. Hence, the flexibility of SCF basis sets (e.g., to allow charge transfer and polarization effects) is essential to obtaining definitive results. However, it does appear that a major part of the microscopic solvent-solute interactions to be described can be handled using techniques such as described here.

**Acknowledgment.** The authors would like to express their appreciation to the University of Kansas for partial support

of the computing time required for these studies. Supported in part by Grants from the Upjohn Company, the National Science Foundation, and the North Atlantic Treaty Organization.

## References and Notes

- (1) K. Morokuma, *J. Chem. Phys.*, **55**, 1236 (1971).
- (2) G. G. Hall, *Proc. R. Soc. London, Ser. A*, **205**, 541 (1951).
- (3) C. C. J. Roothaan, *Rev. Mod. Phys.*, **23**, 69 (1951).
- (4) See, for example, H. Popkie, H. Kistenmacher, and E. Clementi, *J. Chem. Phys.*, **59**, 1325 (1973).
- (5) See, for example, A. Pullman and B. Pullman, *Q. Rev. Biophys.*, **7**, 4 (1975), and reference contained therein. See also ref 4, 6-18.
- (6) H. Kistenmacher, G. C. Lie, H. Popkie, and E. Clementi, *J. Chem. Phys.*, **61**, 546 (1974), and references contained therein.
- (7) H. J. R. Weintraub and A. J. Hopfinger, Proceedings of the 7th Jerusalem Symposium on Molecular and Quantum Pharmacology, B. Pullman, Ed., in press, and references contained therein.
- (8) R. Grohn, *Ark. Fys.*, **21**, 13 (1962).
- (9) G. Nementhy and H. A. Scheraga, *J. Chem. Phys.*, **36**, 3382 (1962).
- (10) A. Rahman and F. Stillinger, *J. Chem. Phys.*, **55**, 3336 (1971).
- (11) M.-J. Huron and P. Claverie, *Chem. Phys. Lett.*, **9**, 194 (1971).
- (12) N. Salaj, *Acta Chem. Scand.*, **23**, 1534 (1969).
- (13) J. E. Del Bene, *J. Chem. Phys.*, **62**, 1961 (1975).
- (14) R. Bonaccorsi, C. Petrongolo, E. Scrocco, and J. Tomasi, *Theor. Chim. Acta*, **20**, 331 (1971).
- (15) G. Alagona, R. Cimiraglia, E. Scrocco, and J. Tomasi, *Theor. Chim. Acta*, **25**, 103 (1972).
- (16) G. Alagona, A. Pullman, E. Scrocco, and J. Tomasi, *Int. J. Pept. Res.*, **5**, 251 (1973).
- (17) G. N. J. Port and A. Pullman, *FEBS Lett.*, **31**, 70 (1973).
- (18) For a discussion of relevant experimental work in this area, see, for example, P. Kebarle, "Ion Molecule Reactions", J. L. Franklin, Ed., Plenum Press, New York, N.Y., 1972, Chapter 7, p 315.
- (19) See J. L. Nelson, C. C. Coff, and A. A. Frost, *J. Chem. Phys.*, **60**, 712 (1974), and earlier references contained therein.
- (20) G. G. Hall, *Chem. Phys. Lett.*, **6**, 501 (1973).
- (21) A. D. Tait and G. G. Hall, *Theor. Chim. Acta*, **31**, 311 (1973).
- (22) L. L. Shipman, *Chem. Phys. Lett.*, **31**, 361 (1975).
- (23) T. D. Davis, R. E. Christoffersen, and G. M. Maggiora, *J. Am. Chem. Soc.*, **97**, 1347 (1975), and references contained therein for a description of the molecular fragment method.
- (24) M. Dreyfus, B. Maigret, and A. Pullman, *Theor. Chim. Acta*, **17**, 109 (1970).
- (25) See, for example, P. A. Kollman and L. C. Allen, *J. Am. Chem. Soc.*, **93**, 4991 (1971).
- (26) See, for example, D. Spangler, R. McKinney, G. M. Maggiora, L. L. Shipman, and R. E. Christoffersen, *Chem. Phys. Lett.*, **36**, 427 (1975), for an example of an ab initio SCF calculation on a 340-electron system using FSGO basis orbitals.